Elucidation of the Ebola Virus VP24 Cellular Interactome and Disruption of Virus Biology through Targeted Inhibition of Host-Cell Protein Function

Isabel García-Dorival,[†,‡] Weining Wu,[†] Stuart Dowall,[§] Stuart Armstrong,[†,‡] Olivier Touzelet,[†] Jonathan Wastling,[†,‡] John N. Barr,[∥] David Matthews,[⊥] Miles Carroll,[‡,§] Roger Hewson,*[,‡,§] and Julian A. Hiscox*[,†,‡]

[†]Department of Infection Biology, Institute of Infection and Global Health, University of Liverpool, Liverpool L3 5RF, United Kingdom

[‡]NIHR Health Protection Research Unit in Emerging and Zoonotic Infections, Liverpool L69 7BE, United Kingdom
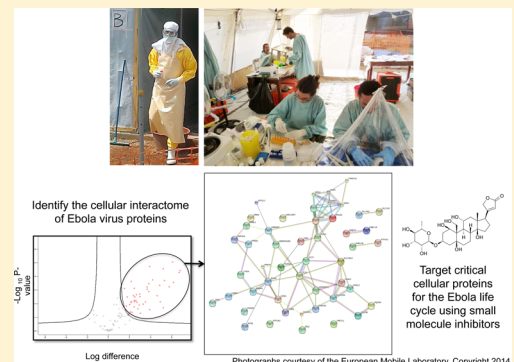
[§]Public Health England, Porton Down, Salisbury SP4 0JG, United Kingdom

[∥]School of Molecular and Cellular Biology, Faculty of Biological Science, University of Leeds, Leeds LS2 9JT, United Kingdom

[⊥]School of Cellular and Molecular Medicine, University of Bristol, Bristol BS8 1TD, United Kingdom

ABSTRACT: Viral pathogenesis in the infected cell is a balance between antiviral responses and subversion of host-cell processes. Many viral proteins specifically interact with host-cell proteins to promote virus biology. Understanding these interactions can lead to knowledge gains about infection and provide potential targets for antiviral therapy. One such virus is Ebola, which has profound consequences for human health and causes viral hemorrhagic fever where case fatality rates can approach 90%. The Ebola virus VP24 protein plays a critical role in the evasion of the host immune response and is likely to interact with multiple cellular proteins. To map these interactions and better understand the potential functions of VP24, label-free quantitative proteomics was used to identify cellular proteins that had a high probability of forming the VP24 cellular interactome. Several known interactions were confirmed, thus placing confidence in the technique, but new interactions were also discovered including one with ATP1A1, which is involved in osmoregulation and cell signaling. Disrupting the activity of ATP1A1 in Ebola-virus-infected cells with a small molecule inhibitor resulted in a decrease in progeny virus, thus illustrating how quantitative proteomics can be used to identify potential therapeutic targets.

Identify the cellular interactome of Ebola virus proteins

Target critical cellular proteins for the Ebola life cycle using small molecule inhibitors

Photographs courtesy of the European Mobile Laboratory. Copyright 2014.

KEYWORDS: Ebola virus, VP24 protein, label free proteomics, proteomics, virus, antiviral, inhibitor, interactome

■ INTRODUCTION

Ebola virus causes severe hemorrhagic fever in humans and nonhumans primates. Because of the high mortality rate, potential transmission from person-to-person contact, and the lack of approved vaccines or antiviral therapies, Ebola viruses are classified as hazard group 4 pathogens by the Advisory Committee on Dangerous Pathogens (ACDP). The *Ebolavirus* genus is one of three genera of the family *Filoviridae*. Currently, this genus is composed of five alternative species of the Ebola virus, which are associated with different pathogenicity and case fatality rates. Zaire Ebola virus (EBOV) is the most pathogenic for humans and causes sporadic outbreaks with fatality rates reaching up to 90%, while Reston Ebola virus (RESTV) is not pathogenic for humans. However, RESTV can cause viral hemorrhagic fever in nonhuman primates and illustrates the potential zoonotic threat of Ebola virus.[1−3] Ebola virus outbreaks occur irregularly, with the most recent outbreak occurring in West Africa in 2014, with fatality rates currently over 60%.

Ebola virus is an enveloped nonsegmented negative single-stranded RNA virus with a genome of 19kb in length consisting of seven genes encoding eight proteins: nucleoprotein (NP), virion protein (VP) 35, VP40, glycoprotein (GP), VP30, VP24, and the RNA-dependent RNA polymerase (L). The combination and action of these gene products and their interactions with the host cell cause the severe hemorrhagic fever. One of the proteins thought to contribute to disease pathology is VP24 and may be a major factor in virulence.[4] This protein is considered a secondary matrix protein as only a small amount of VP24 is incorporated into viral particles. However, VP24 has affinity for the plasma membrane and is associated with the envelope of the virion. VP24 has been shown to have several

functions, including an involvement in viral nucleocapsid formation and the regulation of replication.[5,6]

Critically, VP24 is also involved in modulation of the host response to infection through evasion of the host immune response. VP24 may disrupt interferon signaling by binding to karyopherin-α (KNP-α),[7] which blocks the nuclear accumulation of tyrosine-phosphorylated STAT1 (PY-STAT).[8] STAT1 is a major signaling molecule involved in initiating the antiviral response.[9] Nuclear translocation of STAT1 is essential for transcriptional activation of numerous interferon responsive genes. VP24 can also inhibit IFN-α/β- and IFN-γ-induced gene expression.[10] The mechanism of action through which VP24 modulates the immune response is unknown. However, other work suggested that VP24 may be structurally similar to importin-α/β and exportin.[11] Thus, VP24 may be involved in the mimicry of host transporter/cargo interactions.[11,12] Mutations in VP24 have been linked to the adaptation of Zaire Ebola virus in mice and guinea pigs to produce lethal disease.[13−15]

Therefore, VP24 may form critical protein−protein interactions with host-cell proteins to modulate host-cell pathways; this is the case of the interaction of VP24 with karyopherin, which is required for the inhibition of the interferon-signaling pathway. Elucidating these interactions in detail would provide a deeper understanding of Ebola virus infection and also potentially present antiviral chemo-therapeutic targets to disrupt virus biology.

To determine which cellular proteins or complexes interact with VP24 and to predict function, we have used high-affinity purification coupled to a label-free mass-spectrometry-based approach. Using conservative selection criteria, approximately 50 cellular proteins were identified that had a high probability of interacting with VP24. Some of the candidate proteins had been identified in previous analyses, confirming that our approach was able to identify known interactions, thus increasing confidence that the analysis was capable of identifying new cellular proteins in the same experiment. One of the novel hits identified was sodium/potassium-transporting ATPase subunit alpha-1 (ATP1A1). This enzyme can be inhibited by the small-molecule inhibitor ouabain, which is used in the treatment of heart failure. We used this drug in experiments to inhibit the function of ATP1A1 in cells infected with Ebola virus. The data indicated that progeny virus decreased in treated infected cells compared with untreated infected cells.

■ EXPERIMENTAL PROCEDURES

EGFP-VP24 and VP24-EGFP Construction

Codon-optimized (for expression in human cells) cDNA sequence encoding Zaire EBOV Mayinga Strain 1976 VP24 protein (NCBI reference sequence number: NP_066250.1) was cloned into the pEGFP-C1 and pEGFP-N1 vectors to generate Zaire EBOV VP24 with C-terminal EGFP tag and N-terminal EGFP tag; the plasmid sequences were confirmed by sequencing.

Cell Culture and Transfections

HEK 293T cells were grown in Dulbecco's modified Eagle's medium (DMEM; Sigma-Aldrich) supplemented with 10% fetal bovine serum (FBS; Sigma-Aldrich) and 1% penicillin-streptomycin (Sigma-Aldrich) at 37 °C with 5% CO_2. To transfect 293T cells, two 145 cm^2 dishes were seeded with 4×10^6 cells 24 h prior to calcium phosphate transfection with 25.6

μg of plasmid DNA encoding EGFP, EGFP-VP24, and VP24-EGFP, respectively. After 24 h post-transfection the cells were harvested, lysed, and immunoprecipitated using a GFP-Trap (Chromotek).

EGFP Coimmunoprecipitations

EGFP-VP24, VP24-EGFP, and EGFP immunoprecipitations were performed using a GFP-Trap_A (Chromotek), and cell pellet was resuspended in 200 μL of lysis buffer (10 mM Tris/Cl pH 7.5; 150 mM NaCl; 0.5 mM EDTA; 0.5%NP40) supplemented with Halt Protease Inhibitor Cocktail EDTA-Free (Thermo Scientific) and incubated for 30 min on ice. The lysate was clarified by centrifugation at 14 000g and diluted five-fold with dilution buffer (10 mM Tris/Cl pH 7.5; 150 mM NaCl; 0.5 mM EDTA) supplemented with Halt Protease Inhibitor Cocktail EDTA-Free (Thermo Scientific). The GFP-Trap agarose beads were equilibrated with ice-cold dilution buffer supplemented with Halt Protease Inhibitor Cocktail EDTA-Free (Thermo Scientific) and then incubated with diluted cell lysate overnight at 4 °C on a rotator, followed by centrifugation at 2700g for 2 min. The bead pellet was washed two times with wash buffer (10 mM Tris/Cl pH 7.5; 150 mM NaCl; 0.5 mM EDTA) supplemented with Halt Protease Inhibitor Cocktail EDTA-Free (Thermo Scientific). After the removal of wash buffer the beads were resuspended with 25 μL of elution buffer (200 mM Glycine pH 2.5) and incubated for 10 min at room temperature in a thermal shaker to elute bound proteins; the beads were then collected by centrifugation, and the eluted proteins were transferred to a 1.5 mL centrifuge tube. This step was repeated four times to ensure the maximum elution and all of the eluates were combined; 10 μL of Tris-base buffer (pH 10.4) was added to neutralize the eluate. Immunoprecipitated samples were then analyzed using label-free mass spectrometry.

Reverse Coimmunoprecipitation

Immunoprecipitations for Karyopherin α6 and Lamin B1 were performed using the immobilized recombinant protein G resin (Generon) and specific antibodies against karyopherin α6 (E-11) (Santa Cruz Biotechnology; sc-390055) and Lamin B1 (ZL-5) (Santa Cruz Biotechnology; sc-56145). cell pellets were incubated for 30 min on ice with 200 μL of lysis buffer; the lysate was clarified by centrifugation and diluted five-fold with dilution buffer prior to adding 2 μg of the primary antibody and then incubated at 4 °C on a rotator for 2 h. The protein G resin (Generon) was equilibrated with ice-cold dilution buffer and then incubated at 4 °C on a rotator with diluted cell lysate containing the antibody overnight at 4 °C on a rotator, followed by centrifugation at 2700g for 2 min to remove nonbounds. The wash and elution steps were preformed as previously described in GFP coimmunoprecipitation.

Label-Free Mass Spectrometry

Eluted samples were diluted two-fold with 25 mM ammonium bicarbonate. Rapigest (Waters) was added to a final concentration of 0.05% (w/v), and the sample was heated to 80 °C for 10 min. Proteins were reduced with 3 mM dithiothreitol (Sigma) at 60 °C for 10 min, then alkylated with 9 mM iodoacetimide (Sigma) at room temperature for 30 min in the dark. Proteomic grade trypsin (Sigma) was added (0.2 μg), and samples were incubated at 37 °C overnight. The Rapigest was removed by adding TFA to a final concentration of 1% (v/v) and incubating at 37 °C for 2 h. Peptide samples were centrifuged at 12 000g for 60 min (4 °C) to remove

precipitated Rapigest. Each digest was concentrated and desalted using C18 Stage tips (Thermo Scientific), then dried down using a centrifugal vacuum concentrator (Jouan) and resuspended in a 0.1% (v/v) TFA, 3% (v/v) acetonitrile solution.

Peptide mixtures (2 μL) were analyzed by online nano flow liquid chromatography using the nanoACQUITY-nLC system (Waters MS technologies, Manchester, U.K.) coupled to an LTQ-Orbitrap Velos (Thermo Fisher Scientific, Bremen, Germany) mass spectrometer equipped with the manufacturer's nanospray ion source. The analytical column (Nano ACQUITY UPLCTM BEH130 C18 15 cm × 75 μm, 1.7 μm capillary column) was maintained at 35 °C and a flow-rate of 300nL/min. The gradient consisted of 3−40% acetonitrile in 0.1% formic acid for 50 min then a ramp of 40−85% acetonitrile in 0.1% formic acid for 3 min. Full-scan MS spectra (m/z range 300−2000) were acquired by the Orbitrap at a resolution of 30 000. Analysis was performed in data-dependent mode. The top-20 most intense ions from MS1 scan (full MS) were selected for tandem MS by collision-induced dissociation (CID), and all product spectra were acquired in the LTQ ion trap.

Label-Free Analysis

Label-free quantitation was performed using MaxQuant (MQ) software (version 1.3.0.5.) with its internal search engine Andromeda. Precursor mass and fragment mass were searched with mass tolerance of 6 ppm and 0.5 Da, respectively. All other settings were default. The search included variable modifications of methionine oxidation and N-terminal acetylation and fixed modification of carbamidomethyl cysteine. Enzyme specificity was set to trypsin, minimal peptide length was set to seven amino acids, and a maximum of two mis-cleavages was allowed. The false discovery rate (FDR) was set to 0.01 for peptide and protein identifications. The Andromeda search engine was configured for a database containing human proteins (Uniprot release-2013_03) and VP24 GFP constructs (56601 entries). The MQ software further included a decoy database as well as containing common contaminants to determine the FDR and to exclude false-positive hits due to contamination by proteins from different species. For LFQ analysis, "multiplicity" was set to one. Feature matching between raw files was enabled using a retention time window of 2 min. "Discard unmodified counterpart peptides" was unchecked. Only unmodified and unique peptides were utilized. Averaged LFQ intensity values were used to calculate protein ratios.

Bioinformatics Analysis

Label-free mass spectrometry results were processed and analyzed using the Perseus software (MaxQuant); this software was used to perform the statistical analysis and to differentiate background proteins (those cellular proteins that interacted with EGFP alone) from interacting proteins (those cellular proteins that interacted with EGFP-VP24 or VP24-EGFP). LFQ intensity values were analyzed using a T-Test. A volcano plot graphic and a table were generated showing the statistical significant proteins, those proteins that had a high probability of interacting with VP24. The String 9.05. program was used to predict the protein−protein interactions of the statistically significant proteins and also to group proteins according to function.

Western Blot Analysis

Beads were then resuspended and boiled in 100 μL of 2× SDS-sample buffer at 95° for 10 min to elute the bound proteins. The beads were then collected by centrifugation, and SDS-PAGE was preformed with the supernatant (elution faction). 10% SDS polyacrylamide gels were used to perform the SDS-PAGE; then, gels were transferred to PVDF membranes (Millipore) using a semidry transfer system. Transferred membranes were blocked in 5% skimmed milk powder dissolved in TBS-0.1% Tween (TBS-T) (50 mM Tris-HCl (pH8.3), 150 mM NaCl, and 0.5% (v/v) Tween-20) buffer for 60 min at room temperature. Primary antibody was diluted 1:1000 in blocking buffer and then incubated at 4 °C overnight; antibodies used against GFP (Santa Cruz Biotechnology; sc-8334), karyopherin α6 (E-11) (Santa Cruz Biotechnology; sc-390055), Lamin B1 (ZL-5) (Santa Cruz Biotechnology; sc-56145), and Na$^+$/K$^+$-ATPase α (H-3) (Santa Cruz Biotechnology; sc-48345) were from Santa Cruz, and anti-VDAC1/porin antibody was from Abcam (Abcam; ab14734). After three washes, blots were incubated with appropriate HRP secondary antibody diluted in blocking buffer at a 1:2000 for 1 h at room temperature. Blots were developed using enhanced chemiluminesense reagent (BioRad) and detected using a BioRad Imaging system.

Virus Infection and Treatment with Inhibitor

MRC-5 human fetal lung cells (European Collection of Cell Cultures; 05081101) were maintained in Leibovitz's L-15 media (Invitrogen; 31415-086) supplemented with 10% fetal bovine serum (Sigma; F9665). Media was removed from the cell monolayers, and the cells were infected with Ebola Zaire virus (strain ME718) at a multiplicity of infection of ∼0.1, with virus left to adsorb for 1 h at 37 °C. ME718 was isolated during an outbreak in October 1976 (WHO International Commission, 1978). It was sourced from an acute phase serum sample obtained from a 42-year-old Belgian nun (Sister M.E.) who became ill on September 23, 1976, in Yambuku, Equateur Province Zaire. This strain is equivalent to the Mayinga strain, as Sister M.E. nursed Sister Mayinga (who the strain is named after) and most likely contracted her infection. Leibovitz's L-15 media containing 2% fetal bovine serum was added, and the infected cells were incubated at 37 °C for 1 h. In triplicate flasks, Ouabbain Octahydrate (Sigma; O3125) was added to the media to a final concentration of 20 nM; a further three flasks were left as an untreated control. At 24 and 48 h postinfection, a sample of media from each flask was added to AVL inactivation buffer (Qiagen; 19073) prior to removal from the Containment Level 4 (CL4) laboratory for nucleic acid extraction. The QIAamp Viral RNA Mini Kit from Qiagen (cat. no. 52904) was used for nucleic acid extraction, as this facilitated transport of the nucleic acid samples from CL4 to CL2. Following the extraction of viral RNA, the cDNA was synthesized using specific primers against the gene encoding the nucleoprotein of Zaire Ebola virus. The cDNA was synthesized using the Thermo Script RT-PCR System from Invitrogen (cat. no. 11146-024) following the manufacturer's instructions. PCR was performed with Paq5000 DNA polymerase (Agilent Technologies) (data not shown). Finally, a qPCR was performed to compare the RNA levels in the infected cells treated and untreated with Ouabain experiment. This was performed with the iTaq Universal SYBR Green Supermix (BIO RAD).

■ RESULTS

Expression of VP24 in 293T Cells

To obtain a more complete picture of the interaction partners of VP24, we used quantitative proteomics coupled to an immunoprecipitation strategy based on expressing VP24 as an EGFP-fusion in human 293-T cells and utilizing a GFP-trap to selectively precipitate the fusion protein and interacting partners (Figure 1A). 293-T cells are derived from embryonic kidney cells and were chosen due to their ability to sustain Ebola virus replication, their high transfection efficiencies using calcium-phosphate, and the well-annotated human databases that aid with protein identification and function assignment. To identify interacting cellular partners specific for VP24, we used label-free LC−MS/MS to analyze binding partners from cells expressing either EGFP or the EGFP-VP24 or VP24-EGFP fusion proteins. Subsequent comparison of the immunoprecipitated interacting partners from these conditions allowed the identification of cellular components that specifically bound to the VP24 moiety within the EGFP/VP24 fusion protein. This general approach has been shown to improve sensitivity and allow discrimination of specific from nonspecific interactions with the target protein[16,17] and can be readily applied to the analysis of the cellular interactomes of viral proteins.[18−20]

To identify cellular proteins that interact with VP24, we cloned the gene encoding EGFP either 5′ or 3′ of a gene encoding codon-optimized VP24 from a virus similar to the Zaire EBOV, Mayinga Strain 1976, such that when the construct was transfected in cells the EGFP moiety was expressed as either an N- or C-terminal fusion of VP24, respectively. In this way, we mitigated against potential nonbinding to cellular targets caused by steric hindrance of the EGFP moiety. Proteins were precipitated using the anti-EGFP antibody, and both input (cell lysate) and eluted fraction were compared using immunofluoresence (Figure 1B) and Western blot (Figure 1C). The data indicated that both EGFP-VP24 and VP24-EGFP were expressed with high efficiency at the expected molecular weight (∼55 kDa).

Identification of the Potential Cellular Interacting Partners of VP24

EGFP-VP24, VP24-EGFP, and EGFP were then overexpressed in 293T cells, and the cellular binding partners were immunoprecipitated using the GFP-trap. These proteins were identified by mass spectrometry. To differentiate those cellular proteins that formed specific interactions with VP24 versus those proteins that interacted with EGFP or formed nonspecific interactions with the binding matrix, we repeated the immune precipitations and mass spectrometry five times. Approximately 600 cellular proteins were initially identified and quantified, which represented both the specific and nonspecific interactions. To differentiate between these possibilities, we took several conservative processing steps. The 15 data sets were analyzed by the Perseus software algorithm. Proteins identified by a single peptide were removed, and a p value was set at <0.01 for the t-test analysis, where theoretically only 1:100 proteins were misidentified. The data were then organized in the form of volcano plots for EGFP-VP24 and VP24-EGFP (Figure 2A,B, respectively). These show P values ($-\log_{10}$) for confidence in peptide identification versus fold difference in binding of a protein between the VP24 fusion protein and EGFP only. Dots represent individual proteins. Those dots inside the volcano plots represent proteins that did not associate with VP24 with statistical significance. Proteins that
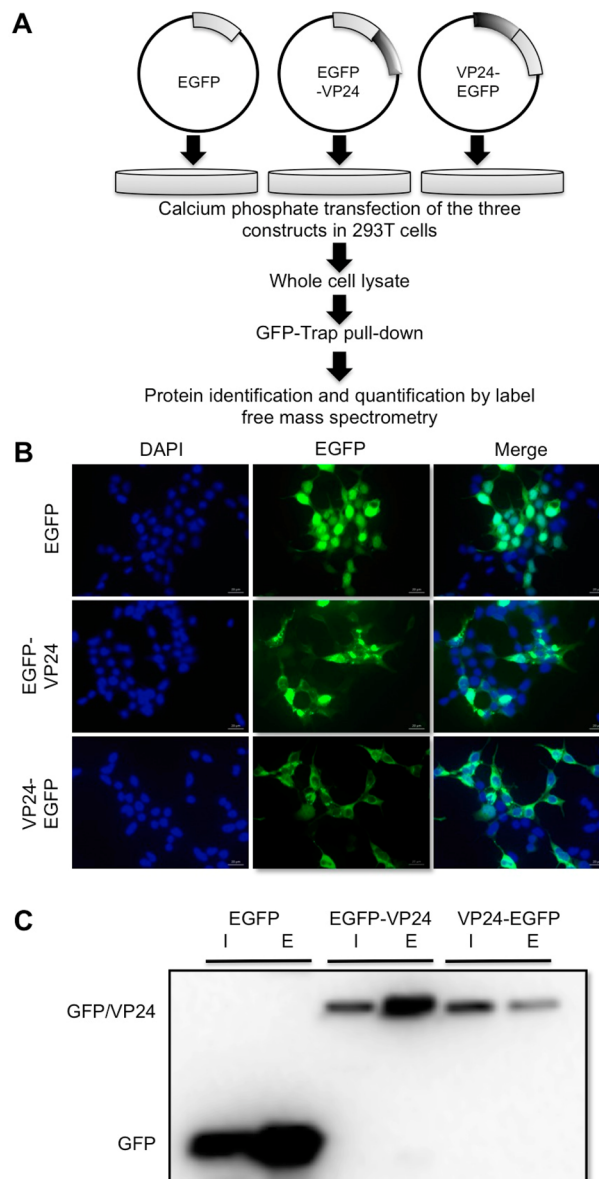

Figure 1. Expression of VP24 in 293T cells. (A) Schematic representation of the methodology used in this study. HEK 293T cells were grown in DMEM supplemented with 10% FBD and 1% penicillin-streptomycin at 37 °C with 5% CO2. Two 145 cm² dishes were seeded with 4×10^6 cells 24 h prior to calcium phosphate transfection with 25.6 μg of plasmid DNA encoding EGFP, EGFP-VP24, and VP24-EGFP, respectively. 24 h post-transfection the cells were harvested, lysed, and immunoprecipitated using a GFP-Trap (Chromotek). Label-free mass spectrometry analysis on the eluted samples was then carried out. (B) Expression of VP24-EGFP, EGFP-VP24, and EGFP in 293T cells was confirmed by immunofluorescence using confocal microscopy and DAPI (blue) to counterstain the nucleus; the panels show that expression of two constructs were similar (however, EGFP-VP24 shows a higher expression than VP24-EGFP) and that approximately 50% of cells were transfected. (C) Analysis of the pull-down products using a Western blot confirm the presence of EGFP-VP24, VP24-EGFP, and EGFP with the expected molecular weight, confirming the expression of these proteins in 293T cells.

had a binding ratio greater than 2 and were statistically significant are shown in the right-hand quadrant. For EGFP-VP24 and VP24-EGFP, 48 and 51 proteins (Table 1),
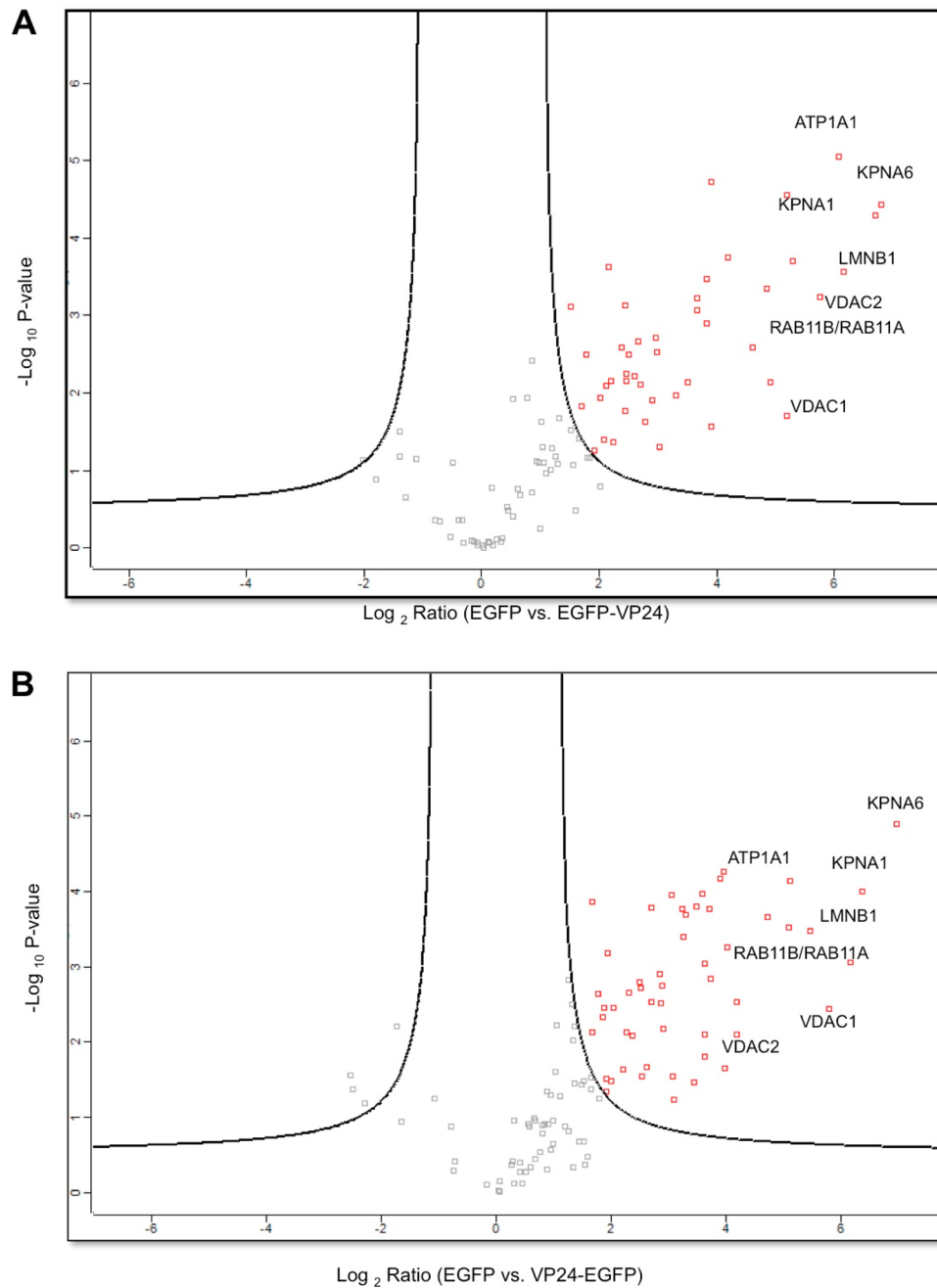
Figure 2. Volcano plot representing results of the label-free pull-down of EGFP-VP24 (A) or VP24-EGFP (B) versus the control EGFP performed in triplicate. For any potential protein interaction partner with VP24, the value of its abundance coimmunoprecipitated with EGFP-VP24 or VP24-EGFP was compared with the value of coimmunoprecipitated with EGFP alone. The logarithmic ratio of protein intensities is plotted against the negative logarithmic p values of the t test. The dashed curve indicates the region of significant interactions with a false discovery rate of 1%, and the red dots in the upper right corners are the proteins that have the highest probability of interacting with VP24.

respectively, were identified as interacting with statistical significance. Both fusion proteins had 40 proteins identified in common; 8 proteins were unique for EGFP-VP24 and 11 proteins were unique for VP24-EGFP. A map of these protein–protein interactions was performed using the String Algorithm (version 9.05) and is presented in Figure 3.

Cellular proteins that had a higher statistical likelihood of associating with VP24 included importin subunit alpha 1 and 6 (karyopherin-α1 and karyopherin-α6), lamin B1, VDAC-1, and ATP1A1. Importin α1 has been previously shown to interact with VP24[8] and therefore indicated that our approach identified

known interactions and increased confidence in the analysis of cellular proteins found in the same experiment. Comparison of proteins identified as interacting with VP24 and their abundance in an average human cell (data taken from PaxDb: Protein Abundance Across Organisms database) (Table 1) indicated that the likelihood of binding was not proportional to their abundance in a cell, thus increasing confidence that the amount of binding was not merely a reflection of overall protein abundance.

Table 1. Cellular Proteins That Have a Higher Probability of Forming Protein–Protein Interactions with VP24[a]

(A) Significant Proteins That Interact with EGFP-VP24

#	protein identifier	gene names	protein names	peptides	unique peptides	−Log P value	fold change	PEP	SC (%)	abundance (ppm)	function	subcellular location
1	P20700; E9PBF6	LMNB1	lamin-B1	40	36	7.01	6.7	0	61.3	105 ppm (top 5%)	Lamins are components of the nuclear lamina, a fibrous layer on the nucleoplasmic side of the inner nuclear membrane.	nucleus, cytoskeleton
2	O60684; F5GYL8	KPNA6	importin subunit alpha-7	16	12	6.5	6.1	4.89×10^{-243}	40.5	4.51 ppm	Functions in nuclear protein import as an adapter protein for nuclear receptor KPNB1.	cytosol, nucleus
3	P52294; C9JYI4	KPNA1	importin subunit alpha-5	13	10	6.7	6.0	7.9×10^{-159}	29.2	5.90 ppm	Functions in nuclear protein import as an adapter protein for nuclear receptor KPNB1.	cytoplasm, nucleus
4	Q15907; P62491	RAB11B;RAB11A	Ras-related protein Rab-11B	6	6	7.1	5.8	1.44×10^{-86}	22.9	42.0 ppm (top 25%)	Member RAS oncogene family; Modulates endosomal trafficking	cell membrane, endosome
5	F5H3A1; P05023	ATP1A1	sodium/potassium-transporting ATPase subunit alpha-1	23	21	7.7	5.6	0	28	46.8 ppm (top 25%)	This is the catalytic component of the active enzyme, which catalyzes the hydrolysis of ATP coupled with the exchange of sodium and potassium ions across the plasma membrane.	cell membrane, endosome, ER
6	P39687; F2Z3H3	ANP32A	acidic leucine-rich nuclear phosphoprotein 32 family member A	6	5	5.8	5.6	1.72×10^{-67}	27.7	305 ppm (top 5%)	Implicated in a number of cellular processes, including proliferation, differentiation and caspasa dependent/independent apoptosis.	ER, nucleus, cytoplasm
7	P16615; Q93084	ATP2A2	sarcoplasmic/endoplasmic reticulum calcium ATPase 2	15	15	5.3	5.1	4.61×10^{-133}	20.2	30.1 ppm (top 25%)	TPase, Ca++ transporting, cardiac muscle.	cell membrane, ER
8	P21796; C9JI87	VDAC1	voltage-dependent anion-selective channel protein 1	10	10	2.9	4.9	2.03×10^{-168}	44.2	370 ppm (top 5%)	Forms a channel through the mitochondrial outer membrane and also the plasma membrane.	mitochondrion, cell membrane
9	P35613; A6NJW1	BSG	basigin	7	7	5.4	4.9	1.81×10^{-124}	21.8	126 ppm (top 10%)	Plays pivotal roles in spermatogenesis, embryo implantation, neural network formation and tumor progression.	cell membrane
10	F8WCY5; Q14257	RCN2	reticulocalbin-2	7	7	7.1	4.5	2.98×10^{-83}	26.3	2.74 ppm	EF-hand calcium binding domain; Not known. Binds calcium	ER
11	Q09028; B4DRT0	RBBP4	histone-binding protein RBBP4	8	5	3.3	4.3	4.44×10^{-82}	22.8	67.4 ppm (top 25%)	Retinoblastoma binding protein 4	nucleus
12	P45880; B4DKM5	VDAC2	voltage-dependent anion-selective channel protein 2	9	9	3.6	4.2	1.2×10^{-78}	54.4	341 ppm (top 5%)	Forms a channel through the mitochondrial outer membrane that allows diffusion of small hydrophilic molecules.	mitochondrion
13	P51571; A6NLM8	SSR4	translocon-associated protein subunit delta	7	7	5.9	4.0	6×10^{-63}	41	37.5 ppm (top 25%)	Signal sequence receptor, delta (translocon-associated protein delta);	ER
14	P07919	UQCRH	cytochrome b-c1 complex subunit 6, mitochondrial	3	3	4.1	3.84	2.96×10^{-73}	29.7	200 ppm (top 10%)	This is a component of the ubiquinol-cytochrome c reductase complex.	mitochondrion
15	O00264; B7Z1L3	PGRMC1	membrane-associated progesterone receptor component 1	8	7	5.3	3.8	2.33×10^{-60}	19	78.5 ppm (top 25%)	Receptor for progesterone (By similarity)	ER
16	B4DW28; P60866	RPS20	40S ribosomal protein S20	4	4	2.9	3.73	6.92×10^{-35}	28.2	126 ppm (top 25%)	RNA binding, constituent component of the ribosome.	cytoplasm

Table 1. continued

(A) Significant Proteins That Interact with EGFP-VP24

	protein identifier	gene names	protein names	peptides	unique peptides	−Log P value	fold change	PEP	SC (%)	abundance (ppm)	function	subcellular location
17	P50402; Q5HY57	EMD	emerin	5	5	7.3	3.7	4.75×10^{-24}	24.4	8.00 ppm	Stabilizes and promotes the formation of a nuclear actin cortical network.	nucleus, ER
18	P12004	PCNA	proliferating cell nuclear antigen	7	5	3.6	3.7	5.42×10^{-51}	34.5	182 ppm (top 10%)	This protein is an auxiliary protein of DNA polymerase delta and is involved in the control of eukaryotic DNA replication.	nucleus, citoskeleton
19	P05141; P12235	SLC25A5	ADP/ATP translocase 2	13	8	2.7	3.5	1.18×10^{-175}	29.2	213 ppm (top 5%)	Catalyzes the exchange of ADP and ATP across the mitochondrial inner membrane.	membrane
20	P04843; F5H6I5	RPN1	dolichyl-diphosphooligosaccharide–protein glycosyltransferase subunit 1	7	7	4.5	3.4	1.16×10^{-66}	13.5	57.7 ppm (top 10%)	Auxiliary protein of DNA polymerase delta and is involved in the control of eukaryotic DNA replication.	ER
21	P51149; C9J8S3	RAB7A	Ras-related protein Rab-7a	6	6	2.840040609	3.370713043	6.14×10^{-126}	30.4	51.6 ppm (top 10%)	Involved in late endocytic transport. Contributes to the maturation of phagosomes (acidification)	endosome
22	P04844; Q5JYR6	RPN2	dolichyl-diphosphooligosaccharide–protein glycosyltransferase subunit 2/ribophorin II	5	5	4.5	3.4	1.88×10^{-60}	11.9	97.7 ppm (top 10%)	Essential subunit of N-oligosaccharyl transferase enzyme.	ER
23	O43175; Q5SZU1	PHGDH	D-3-phosphoglycerate dehydrogenase	15	15	2.4	3.1	8.01×10^{-223}	36.4	84.6 (top 10%)	Phosphatase deshydrogenase activity	cytoplasm
24	P31689; F5GZ88	DNAJA1	DnaJ homologue subfamily A member 1	6	6	3.6	3.0	9.26×10^{-57}	24.2	54.2 ppm (top 25%)	Co-chaperone of Hsc70. Seems to play a role in protein import into mitochondria	membrane
25	P23396; E9PL09	RPS3	40S ribosomal protein S3	8	8	2.4	2.8	1.45×10^{-104}	30	136 ppm (top 5%)	Structural component of the ribosome	cytoplasm
26	Q13263	TRIM28	transcription intermediary factor 1-beta	6	6	3.9	2.8	3.89×10^{-43}	10.4	56.5 ppm (top 10%)	Nuclear corepressor for KRAB domain-containing zinc finger proteins (KRAB-ZFPs). Mediates gene silencing by recruiting CHD3,)	nucleus
27	B4E2P2; Q9UNL2	SSR3	translocon-associated protein subunit gamma	3	3	1.9	2.7	1.14×10^{-62}	14.6	10.1 ppm	TRAP proteins are part of a complex whose function is to bind calcium to the ER membrane.	Er, membrane
28	P10606	COX5B	cytochrome c oxidase subunit 5B, mitochondrial	4	4	3.8	2.7	2.63×10^{-08}	30.2	14.4 ppm	This protein is one of the nuclear-coded polypeptide chains of cytochrome c oxidase.	mitochondrion
29	F8VVM2; F8VWQ0	SLC25A3	phosphate carrier protein, mitochondrial	4	2	1.9	2.6	1.48×10^{-44}	14.2	40.8 ppm (top 25%)	Transport of phosphate groups from the cytosol to the mitochondrial matrix.	mitochondrion
30	F5H4J7; P08195	SLC3A2	4F2 cell-surface antigen heavy chain	4	4	3.7	2.6	6.55×10^{-52}	9.8	45.3 (top 25%)	Required for the function of light chain amino-acid transporters.	membrane
31	P49755	TMED10	transmembrane emp24 domain-containing protein 10	5	5	2.4	2.5	6.21×10^{-45}	22.4	37.2 ppm (top 25%)	Involved in vesicular protein trafficking	ER, membrane
32	P27708; F8VPD4	CAD	CAD protein; glutamine-dependent carbamoyl-phosphate synthase	6	6	3.8	2.5	4.72×10^{-47}	3.2	10.7 ppm	This protein is a "fusion" protein encoding four enzymatic activities of the pyrimidine pathway (GATase, CPSase, ATCase and DHOase)	cytoplasm, nucleus
33	Q14839; F5GWX5	CHD4	chromodomain-helicase-DNA-binding protein 4	8	8	2.4	2.4	1.09×10^{-56}	6.7	7.83 ppm	Component of the histone deacetylase NuRD complex.	cytoplasm, nucleus

Table 1. continued

(A) Significant Proteins That Interact with EGFP-VP24

	protein identifier	protein names	gene names	peptides	unique peptides	−Log P value	fold change	PEP	SC (%)	abundance (ppm)	function	subcellular location
34	P49411	elongation factor Tu, mitochondrial	TUFM	11	11	1.8	2.3	2.62×10^{-114}	28.3	45.3 ppm (top 10%)	This protein promotes the GTP-dependent binding of aminoacyl-tRNA to the A-site of ribosomes during protein biosynthesis	mitochondrion
35	P78527; E7EUY0	DNA-dependent protein kinase catalytic subunit	PRKDC	10	10	3.41	2.3	1.83×10^{-101}	3.8	34.9 ppm (top 25)	Serine/threonine-protein kinase that acts as a molecular sensor for DNA damage. I	nucleus
36	P22626	heterogeneous nuclear ribonucleoproteins A2/B1	HNRNPA2B1	6	6	3.5	2.2	4.16×10^{-27}	22.9	347 ppm (top 5%)	Involved with pre-mRNA processing.	nucleus
37	Q16531; E7EPB0	DNA damage-binding protein 1	DDB1	6	6	2.8	2.2	3.02×10^{-107}	8.9	22.7 ppm (top 25%)	Required for DNA repair. B	cytoplasm, nucleus
38	P17987; E7ERF2	T-complex protein 1 subunit alpha	TCP1	13	13	4.7	2.1	7.32×10^{-171}	34.9	334 ppm (top 5%)	Molecular chaperone	cytoplasm
39	P08238; Q58FF7	heat shock protein HSP 90-beta	HSP90AB1	14	9	2.5	2.1	2.46×10^{-115}	18.1	713 ppm (top 5%)	Molecular chaperone. Has ATPase activity (By similarity)	cytoplasm
40	P30050	60S ribosomal protein L12	RPL12	5	5	1.9	2.1	1.62×10^{-81}	49.7	425 ppm (top 5%)	Binds directly to 26S rRNA (By similarity)	cytoplasm
41	Q15758; E9PC01	neutral amino acid transporter B(0)	SLC1A5	3	3	4.1	2.1	6.72×10^{-34}	8.3	21.6 ppm (top 25%)	Act as a cell surface receptor for feline endogenous virus RD114, baboon M7 endogenous virus and type D simian retroviruses	membrane
42	Q96TA2; B4DNM1	ATP-dependent zinc metalloprotease YME1L1	YME1L1	4	4	3.5	2.1	2.44×10^{-50}	10.1	14.6 ppm (top 25%)	Putative ATP-dependent protease which plays a role in mitochondrial protein metabolism.	mitochondrion
43	P62879; C9JXA5	guanine nucleotide-binding protein G(I)/G(S)/G(T) subunit beta-2	GNB2	3	3	3.0	1.9	9.24×10^{-17}	11.2	121 ppm (Top 5%)	Guanine nucleotide-binding proteins (G proteins) are involved as a modulator or transducer in various transmembrane signaling systems.	cytoplasm, perinuclear region
44	O15269; Q96IX6	serine palmitoyltransferase 1	SPTLC1	5	5	3.8	1.9	3.87×10^{-91}	14.8	83.1 ppm (top 10%)	The heterodimer formed with SPTLC2 or SPTLC3 constitutes the catalytic core.	ER
45	P07437; F8VW92	tubulin beta chain	TUBB	21	4	3.8	1.8	0	57.4	223 ppm (top 5%)	Tubulin is the major constituent of microtubules.	cytoplasm, cytoskeleton
46	Q8N163; E5RHJ4	cell cycle and apoptosis regulator protein 2, DBIRD complex subunit KIAA1967	KIAA1967	6	6	3.1	1.8	6.22×10^{-92}	10.4	150 ppm (top 5%)	Inhibits SIRT1 deacetylase activity leading to increasing levels of p53/TP53 acetylation and p53-mediated apoptosis.	nucleus
47	Q99832; B8ZZC9	T-complex protein 1 subunit eta	CCT7	3	3	2.3	1.7	6.95×10^{-14}	8.1	116 ppm (top 5%)	Molecular chaperone; assist the folding of proteins upon ATP hydrolysis.	cytoplasm, cytoskeleton
48	P61978; Q5T6W5	heterogeneous nuclear ribonucleoprotein K	HNRNPK	7	7	3.9	1.7	1.48×10^{-60}	21.2	511 ppm (top 5%)	One of the major pre-mRNA-binding proteins.	cytoplasm, nucleus

(B) Significant Proteins That Interact with VP24-EGFP

	protein identifier	protein names	gene names	peptides	unique peptides	−Log P value	fold change	PEP	SC%	abundance (ppm)	function	subcellular location
1	P20700; E9PBF6	lamin-B1	LMNB1	40	36	5.9	6.8	0	61.3	105 ppm (top 5%)	Lamins are components of the nuclear lamina, a fibrous layer on the nucleoplasmic side of the inner nuclear membrane.	nucleus, cytoskeleton
2	O60684; F5GYL8	importin subunit alpha-7; importin subunit alpha	KPNA6	16	12	8.6	6.2	4.89×10^{-243}	40.5	4.51 ppm	Functions in nuclear protein import as an adapter protein for nuclear receptor KPNB1.	cytoplasm, nucleus

Table 1. continued

(B) Significant Proteins That Interact with VP24-EGFP

	protein identifier	protein names	gene names	peptides	unique peptides	−Log P value	fold change	PEP	SC%	abundance (ppm)	function	subcellular location
3	P52294; C9JYI4	importin subunit alpha-1	KPNA1	13	10	6.3	5.97	7.90×10^{-159}	29.2	5.90 ppm	Functions in nuclear protein import as an adapter protein for nuclear receptor KPNB1.	cytoplasm, nucleus
4	Q15907; P62491	Ras-related protein Rab-11B	RAB11B; RAB11A	6	6	6.7	5.4	1.44×10^{-86}	22.9	42.0 ppm (top 25%)	Member RAS oncogene family; Modulates endosomal trafficking	cell membrane, endosome
5	P35613; A6NJW1;	basigin	BSG	7	7	5.2	5.3	1.81×10^{-124}	21.8	126 ppm (top 10%)	Plays pivotal roles in spermatogenesis, embryo implantation, neural network formation, and tumor progression	cell membrane
6	F5H3A1; P05023;	sodium/potassium-transporting ATPase subunit alpha-1	ATP1A1	23	21	9.9	5.3	0	28	46.8 ppm (top 25%)	This is the catalytic component of the active enzyme, which catalyzes the hydrolysis of ATP coupled to the exchange of sodium and potassium ions across the plasma membrane.	cell membrane, endosome, ER
7	Q09028; B4DRT0	histone-binding protein RBBP4	RBBP4	8	5	3.2	4.8	4.44×10^{-82}	22.8	67.4 (top 25%)	Retinoblastoma binding protein 4; Core histone-binding subunit that may target chromatin assembly factors.	nucleus
8	P39687; F2Z3H3	acidic leucine-rich nuclear phosphoprotein 32 family member A	ANP32A	6	5	2.4	4.2	1.72×10^{-67}	27.7	305 ppm (top 5%)	Implicated in a number of cellular processes, including proliferation, differentiation, and caspase dependent/independent apoptosis.	ER, nucleus, cytoplasm
9	F8WCY5; Q14257	reticulocalbin-2	RCN2	7	7	7.9	4.1	2.98×10^{-83}	26.3	2.74 ppm	EF-hand calcium binding domain; Not known. Binds calcium	ER
10	B4DW28; P60866;	40S ribosomal protein S20	RPS20	4	4	3.3	3.9	6.92×10^{-35}	28.2	126 ppm (top 25%)	RNA binding, constituent componet of the ribosome.	cytoplasm
11	P05141; P12235	ADP/ATP translocase 2	SLC25A5	13	8	2.6	3.9	1.18×10^{-175}	29.2	213 ppm (top 5%)	Catalyzes the exchange of ADP and ATP across the mitochondrial inner membrane.	membrane
12	P51571; A6NLM8	translocon-associated protein subunit delta	SSR4	7	7	8.6	3.8	6.00×10^{-63}	41	37.5 ppm (top 25%)	Signal sequence receptor, delta (translocon-associated protein delta).	ER
13	P07919	cytochrome b-c1 complex subunit 6, mitochondrial	UQCRH	3	3	3.9	3.8	2.96×10^{-73}	29.7	200 ppm (top 10%)	This is a component of the ubiquinol-cytochrome c reductase complex	mitochondrion
14	P12004	proliferating cell nuclear antigen	PCNA	7	7	3.4	3.8	5.42×10^{-51}	34.5	182 ppm (top 10%)	This protein is an auxiliary protein of DNA polymerase delta and is involved in the control of eukaryotic DNA replication.	nucleus, citoskeleton
15	P10606	cytochrome c oxidase subunit 5B, mitochondrial	COX5B	4	4	4.0	3.7	2.63×10^{-08}	30.2	14.4 ppm	This protein is one of the nuclear-coded polypeptide chains of cytochrome c oxidase, the terminal oxidase in mitochondrial electron transport.	mitochondrion
16	P50402; Q5HY57	emerin	EMD	5	5	5.9	3.6	4.75×10^{-24}	24.4	8.00 ppm	Stabilizes and promotes the formation of a nuclear actin cortical network.	nucleus, ER
17	P21796; C9JI87	voltage-dependent anion-selective channel protein 1	VDAC1	10	10	3.5	3.5	2.03×10^{-168}	44.2	370 ppm (top 5%)	Forms a channel through the mitochondrial outer membrane and also the plasma membrane.	mitochondrion, cell membrane
18	P16615; Q93084	sarcoplasmic/endoplasmic reticulum calcium ATPase 2	ATP2A2	15	15	5.5	3.5	4.61×10^{-133}	20.2	30.1 ppm (top 25%)	TPase, Ca++ transporting, cardiac muscle	cell membrane, ER
19	P45880; B4DKM5	voltage-dependent anion-selective channel protein 2	VDAC2	9	9	3.5	3.3	1.20×10^{-78}	54.4	341 ppm (top 5%)	Forms a channel through the mitochondrial outer membrane that allows diffusion of small hydrophilic molecules.	mitochondrion
20	O43175; Q5SZU1	D-3-phosphoglycerate dehydrogenase	PHGDH	15	15	2.9	3.2	8.01×10^{-223}	36.4	84.6 (top 10%)	Phosphatase deshydrogenase activity	cytoplasm
21	B4E2P2; Q9UNL2	translocon-associated protein subunit gamma	SSR3	3	3	4.2	3.2	1.14×10^{-62}	14.6	10.1 ppm	TRAP proteins are part of a complex whose function is to bind calcium to the ER membrane and thereby regulate the retention of ER resident proteins.	ER, membrane
22	P49411	elongation factor Tu, mitochondrial	TUFM	11	11	2.9	3.2	2.62×10^{-114}	28.3	45.3 ppm (top 10%)	This protein promotes the GTP-dependent binding of aminoacyl-tRNA to the A-site of ribosomes during protein biosynthesis	mitochondrion

Table 1. continued

(B) Significant Proteins That Interact with VP24-EGFP

	protein identifier	protein names	gene names	peptides	unique peptides	−Log P value	fold change	PEP	SC%	abundance (ppm)	function	subcellular location
23	P04843; F5H6I5	dolichyl-diphosphooligosaccharide–protein glycosyltransferase subunit 1	RPN1	7	7	5.7	3.2	1.16×10^{-66}	13.5	57.7 ppm (top 10%)	Auxiliary protein of DNA polymerase delta and is involved in the control of eukaryotic DNA replication.	ER
24	P23396; E9PL09	40S ribosomal protein S3	RPS3	8	8	3.2	3.1	1.45×10^{-104}	30	136 ppm (top 5%)	Structural component of the ribosome	cytoplasm
25	P04844; Q5JYR6	dolichyl-diphosphooligosaccharide–protein glycosyltransferase subunit 2/ribophorin II	RPN2	5	5	4.5	3.4	1.88×10^{-60}	11.9	97.7 ppm (top 10%)	Essential subunit of N-oligosaccharyl transferase enzymes	ER
26	O00264; B7Z1L3	membrane-associated progesterone receptor component 1	PGRMC1	8	7	6.4	2.9	2.33×10^{-60}	19	78.5 ppm (top 25%)	Receptor for progesterone (by similarity)	ER
27	P31689; F5GZ88	DnaJ homologue subfamily A member 1	DNAJA1	6	6	1.9	2.8	9.26×10^{-57}	24.2	54.2 ppm (top 25%)	Co-chaperone of Hsc70. Seems to play a role in protein import into mitochondria	membrane
28	P49755	transmembrane emp24 domain-containing protein 10	TMED10	5	5	3.7	2.7	6.21×10^{-45}	22.4	37.2 ppm (top 25%)	Involved in vesicular protein trafficking	ER, membrane
29	P51149; C9J8S3	Ras-related protein Rab-7a	RAB7A	6	6	4.8	2.6	6.14×10^{-126}	30.4	51.6 ppm (top 10%)	Involved in late endocytic transport. Contributes to the maturation of phagosomes (acidification)	endosome
30	Q8N163; E5RHJ4	DBIRD complex subunit KIAA1967	KIAA1967	6	6	4.4	2.6	6.22×10^{-92}	10.4	150 ppm (top 5%)	Inhibits SIRT1 deacetylase activity leading to increasing levels of p53/TP53 acetylation and p53-mediated apoptosis.	nucleus
31	P07437; F8VW92	tubulin beta chain	TUBB	21	4	5.5	2.5	0	57.4	223 ppm (top 5%)	Tubulin is the major constituent of microtubules.	cytoplasm, cytoskeleton
32	P17987; E7ERF2	T-complex protein 1 subunit alpha	TCP1	13	13	4.9	2.4	7.32×10^{-171}	34.9	334 ppm (top 5%)	Molecular chaperone; assists the folding of proteins upon ATP hydrolysis.	cytoplasm
33	Q14839; F5GWX5	chromodomain-helicase-DNA-binding protein 4	CHD4	8	8	3.4	2.3	1.09×10^{-56}	6.7	7.83 ppm	Component of the histone deacetylase NuRD complex which participates in the remodeling of chromatin.	nucleus
34	Q9P258	protein RCC2	RCC2	6	6	1.8	2.3	9.96×10^{-36}	15.9	67.00 ppm (top 10%)	Required for completion of mitosis and cytokinesis.	nucleus, cytoplasm
35	Q13263	transcription intermediary factor 1-beta	TRIM28	6	6	1.4	2.2	3.89×10^{-43}	10.4	56.5 ppm (top 10%)	Nuclear corepressor for KRAB domain-containing zinc finger proteins (KRAB-ZFPs). Mediates gene silencing.	nucleus
36	P35268	60S ribosomal protein L22	RPL22	2	2	2.3	2.2	1.22×10^{-20}	30.5	659 ppm (top 5%)	Binds to Epstein–Barr virus small RNAs and to heparin.	cytoplasm
37	Q9Y5M8	signal recognition particle receptor subunit beta	SRPRB	5	5	1.6	2.2	6.04×10^{-40}	26.2	21 ppm (top 25%)	Component of the SRP (signal recognition particle) receptor.	ER, membrane
38	Q96CS3; B4E2M8	FAS-associated factor 2	FAF2	5	5	2.2	2.2	1.14×10^{-93}	18.2	16.8 ppm (top 25%)	May play a role in the translocation of terminally misfolded proteins from the endoplasmic reticulum lumen to the cytoplasm and their degradation by the proteasome.	ER, cytoplasm
39	P35232; C9JW96	prohibitin	PHB	7	7	2.9	2.2	5.73×10^{-82}	30.9	213 ppm (top 5%)	Prohibitin inhibits DNA synthesis. It has a role in regulating proliferation.	membrane, mitochondrion
40	P27708; F8VPD4	CAD protein; glutamine-dependent carbamoyl-phosphate synthase; carbamoyl-transferase; dihydroorotase	CAD	6	6	4.1	2.2	4.72×10^{-47}	3.2	10.7 ppm	This protein is a "fusion" protein encoding four enzymatic activities of the pyrimidine pathway (GATase, CPSase, ATCase, and DHOase)	cytoplasm, nucleus
41	Q15758; E9PC01	neutral amino acid transporter B(0)	SLC1A5	3	3	5.4	2.2	6.72×10^{-34}	8.3	22.8 ppm (top 25%)	Acts as a cell surface receptor for feline endogenous virus RD114, baboon M7 endogenous virus, and type D simian retroviruses.	membrane

Table 1. continued

(B) Significant Proteins That Interact with VP24-EGFP

	protein identifier	protein names	gene names	peptides	unique peptides	−Log P value	fold change	PEP	SC%	abundance (ppm)	function	subcellular location
42	O95831	apoptosis-inducing factor 1, mitochondrial	AIFM1; PDCD8	7	7	3.4	2.1	2.87×10^{-34}	20.4	43.3 ppm (top 10%)	Functions both as NADH oxidoreductase and as regulator of apoptosis. Apoptosis-inducing factor.	mitochondrion, cytoplasm, nucleus
43	Q99832; B8ZZC9	T-complex protein 1 subunit eta	CCT7	3	3	2.0	2.1	6.95×10^{-14}	8.1	116 ppm (top 5%)	Molecular chaperone; assists the folding of proteins upon ATP hydrolysis.	cytoplasm
44	P10412	histone H1.4	HIST1H1E	5	3	2.2	2.1	4.48×10^{-43}	21.5	534 ppm (top 5%)	Histone H1 protein binds to linker DNA between nucleosomes forming the macromolecular structure known as the chromatin fiber.	nucleus
45	Q16531; E7EPB0	DNA damage-binding protein 1	DDB1	6	6	2.6	1.9	3.02×10^{-107}	8.9	22.7 ppm (top 25%)	Required for DNA repair. Binds to DDB2 to form the UV-damaged DNA-binding protein complex (the UV-DDB complex).	cytoplasm, nucleus
46	P48643; E9PCA1	T-complex protein 1 subunit epsilon	CCT5	4	4	2.9	1.9	3.45×10^{-20}	9.1	278 ppm (top 5%)	Molecular chaperone; assists the folding of proteins upon ATP hydrolysis. plays a role, in vitro, in the folding of actin and tubulin	cytoplasm, cytoskeleton
47	P08238; Q58FF7	heat shock protein HSP 90-beta	HSP90AB1	14	9	2.9	1.9	2.46×10^{-115}	18.1	713 ppm (top 5%)	Molecular chaperone. Has ATPase activity (By similarity)	cytoplasm
48	P08708; P0CW22	40S ribosomal protein S17	RPS17; RPS17L	3	3	2.6	1.8	5.71×10^{-42}	37.8	443 ppm (top 5%)	Structural component of ribosome	cytoplasm
49	P78527; E7EUY0	DNA-dependent protein kinase catalytic subunit	PRKDC	10	10	3.7	1.8	1.83×10^{-101}	3.8	52.9 ppm (top 10%)	Serine/threonine-protein kinase that acts as a molecular sensor for DNA damage.	nucleus
50	P11142; E9PKE3	heat shock cognate 71 kDa protein	HSPA8	27	23	5.5	1.7	0	35.3	1362 ppm (top 5%)	Acts as a repressor of transcriptional activation.	cytoplasm
51	P08107; F5GZ62	heat shock 70 kDa protein 1A/1B	HSPA1A; HSPA1B	25	13	5.5	1.4	0	39.8	113 ppm (top 5%)	In cooperation with other chaperones, Hsp70s stabilize preexistent proteins against aggregation.	cytoplasm

[a]Shown are candidate proteins identified using the EGFP-VP24 (A) and VP24-EGFP (B) fusion proteins and identified using label-free quantitative proteomics. Protein identifier, protein name, and gene names are indicated. Total and unique peptides used to identify the protein are indicated. The −Log P value is a comparison of the cellular protein between the VP24 pull down and EGFP, where the higher the number means the higher probability of interacting, and a threshold above 2.0 has been selected. The fold-change or fold-difference between the two conditions the VP24-EGFP or EGFP-VP24 versus the EGFP alone is indicated. PEP is the posterior error probability, and percentage of sequence coverage of the protein identified using the peptides is indicated as SC%. The abundance (ppm) of the protein in an average human cell is listed; data are taken from the PaxDb: Protein Abundance Across Organisms database. Indicated is a brief summary of the function and the subcellular localization of each possible interactor partner.
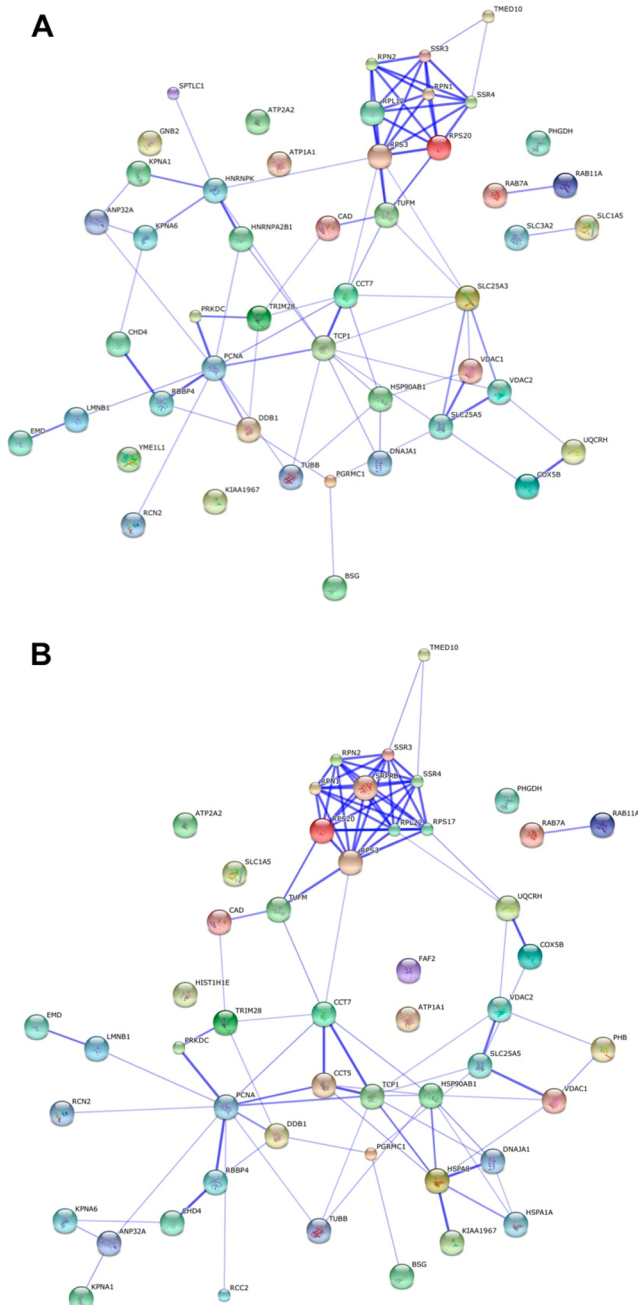
Figure 3. Map showing the group of proteins that interact with VP24: (A) EGFP-VP24 and (B) VP24-EGFP using String 9.1 software. Most of the proteins detected were located in the membranes and in the perinuclear region, as is VP24. In the protein analysis, three main proteins groups were detected: ribosome proteins, mitochondrial proteins, and proteins related to the nucleus.

Validation of VP24-EGFP and EGFP-VP24 Interactions

Selected cellular targets identified in the immune-precipitations to VP24 were then investigated using Western blot as an alternative means of identification (Figure 4A). These targets included karyopherin α6 (as a positive control), ATP1A1, lamin B1, and VDAC-1. The presence of STAT1 was also investigated; even though it had not been identified in the immunoprecipitation, as purified truncated STAT1 and purified truncated VP24 had previously been shown to associate in vitro.[21] Whole cell lysate (input) and eluate (elution) from

Figure 4. Validation of VP24-EGFP and EGFP-VP24 interactions by Western blot analysis. (A) Confirmation of proteins detected in the label free mass spectrometry analysis by Western blot analysis was done in the whole cell lysate or input sample (I) and in the eluate sample (E) for the three different expression constructs. Specific monoclonal antibodies against karyopherin-α6, laminB-1, ATP1A1, VDAC-1, and STAT-1 were used to the detection of the example proteins. The antibody anti-EGFP was used as a control to show the presence of the constructs EGFP-VP24 and VP24-EGFP in the input and in the elution samples. (B) Validation of VP24-EGFP and EGFP-VP4 interactions by reverse immunoprecipitations. To further validate the mass spectrometry results, we performed reverse immunoprecipitations against selected cellular proteins identified by the label-free mass spectrometry analysis. The selected proteins for the validation of the label-free mass spectrometry by using reverse immunoprecipitations were karyopherin α6 and lamin B1; the presence of the protein complex EGFP-VP24 and VP24-EGFP was confirmed using a Western blot analysis and using a specific antibody against EGFP.

separate immunoprecipitations were separated by 1D SDS-PAGE; proteins were then transferred in Western blot and detected using a primary antibody against each selected protein. The data indicated that karyopherin α6, lamin B1, and ATP1A1 associated with both the EGFP-VP24 and VP24-EGFP moieties. By Western blot, VDAC1 appeared to have a greater association for EGFP-VP24 than VP24-EGFP. Although STAT1 could be detected in the input fractions, it was not detected in the immunoprecipitations (Figure 4A).

To further validate the mass spectrometry results and potential interactions between VP24 and cellular proteins, we performed reverse immunoprecipitations against selected cellular targets where antibody combinations allowed. These targets were karyopherin α6 (as a positive control) and lamin B1. VP24-EGFP, EGFP-VP24, or EGFP were expressed in 293T cells and cell lysates were prepared. Immunoprecipitations were performed using specific monoclonal antibodies against karyopherin α6 and lamin B1. Analysis of the pull-down products using a Western blot confirmed the presence of EGFP-VP24, VP24-EGFP, and EGFP in the input and elution fraction. The presence of EGFP-VP24 and VP24-EGFP was
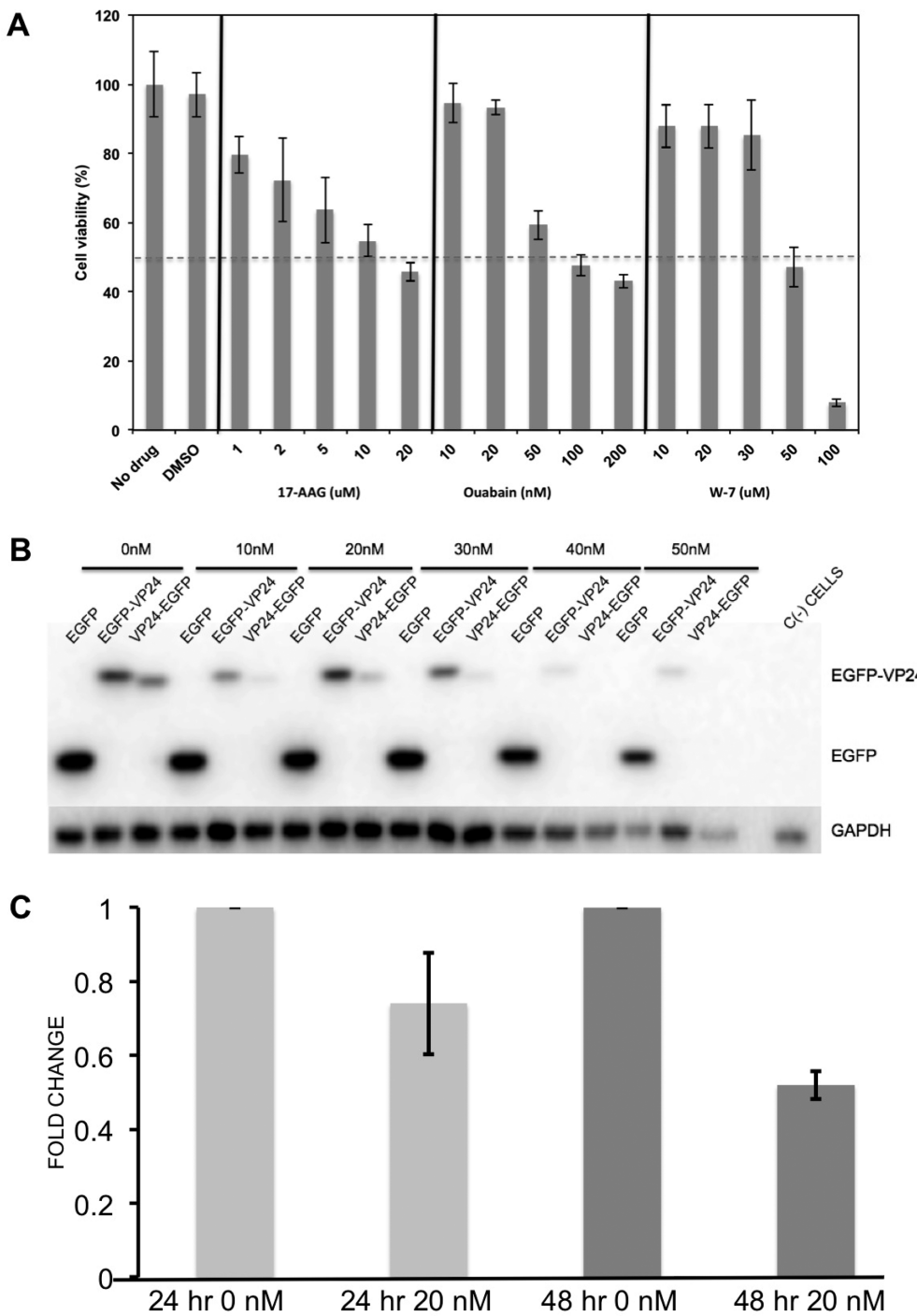
Figure 5. Determining the effect of the ATP1A1 inhibitor ouabain on Ebola virus infected cells. (A) An MTT assay was used to determine cell viability in the absence of drug, the vehicle only control (DMSO), and various concentrations of ouabain and two controls using known small molecule inhibitors that affect the function of target cellular proteins (17-AAG and W-7). The data indicated that 10 and 20 nM ouabain and no apparent effect on cell viability compared with the untreated or vehicle only controls. (B) Stability of EGFP-VP24 and VP24-EGFP compared with the EGFP control were assessed by Western blot in the absence and presence of various concentrations of ouabain. The abundance of GAPDH was also determined. (C) qRT-PCR was used to compare the abundance of viral RNA in RNA purified from supernatant taken from cells infected with Ebola virus at either 24 or 48 h postinfection in the absence (0 nM) or presence of ouabain (20 nM). The data were normalized to viral RNA levels present in infected but untreated cells at 24 and 48 h postinfection.

confirmed using a specific antibody against EGFP (Figure 4B), again validating the forward immunoprecipitations.

Inhibition of ATP1A1 in Ebola Virus Infected Cells

To investigate whether ATP1A1 played a functional role in Ebola virus infected cells, we used the small molecule inhibitor

to ATP1A1, ouabain, to treat human MRC-5 cells infected with EBOV strain ME718 (MOI = 0.1). This fibroblast lung culture was established from a 14-week gestation human male and is a normal diploid cell line that supports the growth of Ebola virus and has been used in antiviral drug screening studies.[22] Cell viability assays were used to determine the affect of different

concentrations of ouabain on cell biology and included two other small-molecule inhibitors (17-AAG and W-7) as positive controls (Figure 5A). The data indicated that both 10 and 20 nM ouabain had no significant effect on cell viability compared with either untreated or cells treated with the vehicle (DMSO) only control. The 20 nM concentration of ouabain also had no apparent effect on the abundance of EGFP-VP24 in treated cells expressing this construct (Figure 5B). Cells were either infected and untreated or infected and treated with 20 nM ouabain to determine the potential effect of this drug on Ebola virus infection. The experiment was repeated in triplicate, and the use of a consistent volume of cell culture supernatant permitted the comparison of the relative abundance of the Ebola virus genome in the supernatant as a proxy measurement for virus particles.[23,24] Therefore, equal volumes of supernatant containing progeny virus were taken at 24 and 48 h postinfection. Viral RNA was then isolated and RNA levels were compared in triplicate using qRT-PCR between each treatment at 24 and 48 h post infection; data were normalized to the level of viral RNA in infected but untreated cells (Figure 5C). Results indicated that infected cells treated with 20 nM ouabain produced less viral RNA compared with infected but untreated cells.

■ DISCUSSION

The genomes of RNA viruses have limited encoding capacity, and therefore viral proteins usually possess multiple functions in the cell and virus life cycle. The elucidation of these interactions provides a better understanding of viral pathogenesis and delivers more options for effective antiviral strategies. Ebola virus VP24 has been shown to have multiple functions in the virus life cycle and therefore would be predicted to interact with a variety of different cellular proteins. Several studies have investigated this with data suggesting that VP24 can interact with karyopherin α, STAT1, and Sec61α.[10,21,25] In this study, affinity tagging coupled to label-free quantitative mass spectrometry was used to identify potential interacting partners of VP24 and reduce or eliminate false-positive interactions. Approximately 50 cellular proteins were identified that had a high probability of interacting with VP24. The majority of proteins identified associated with either EGFP-VP24 or VP24-EGFP. However, some of the cellular proteins identified were unique to the different fusion proteins. This may have been due some of the interactions with the cellular proteins being sterically hindered by the EGFP moiety and emphasized the advantage of using both the N- and C-terminal tagged fusion proteins.

VP24 has affinity for the plasma membrane and has also been observed in the cytoplasm where the protein formed cytoplasmic inclusions.[26] These are the cellular locations of a number of the proteins identified as associating with VP24 (Table 1). The reliability of this mass spectrometry data was confirmed using Western blot analysis and reverse immunoprecipitations against selected cellular proteins. Furthermore, the precipitations and mass spectrometry analysis were repeated five times with independent samples to ensure the reproducibility of the technique and also for the statistical analysis. The immunoprecipitation technique was also optimized for identifying low-affinity and transient interactions by modulating the salt concentration in the washing step.

Karypherin α subunit 6 (KPNA6) and 1 (KPNA1), identified in this study with an average binding ratio of 8 to both EGFP-VP24 and VP24-EGFP, reflected previous work demonstrating

an interaction between EBOV-VP24 and karypherin α subunit 6.[8,10] In addition, as part of a larger viral/host protein study, the interactome of VP24 was determined using tandem affinity purification, and KPNA6 and other karypherins were identified as part of 48 cellular proteins that potentially interacted with VP24.[27] Proteins in common with this previous work and recorded in our analysis as having a greater than two-fold abundance with either EGFP-VP24 or VP24-EGFP were ANP32A, ANP32B, CCAR2 (KIAA1967), CGGBP1, HNRNPL, HNRNPU, KPNA1, KPNA6, MYO5A, POM121C, PRKCSH, RPS27, RPS27L, SLC25A3, TUB1C, and TUBB, 28 proteins were not detected in our study, and three proteins (EEF1A1, EEF1A2, and SPOP) were identified as proteins that formed background/nonspecific interactions.

In the present study, no interaction was detected between VP24 and STAT1 using the mass spectrometry approach, and this was confirmed by Western blot. Likewise, no interaction between VP24 and STAT1 was described in the tandem affinity approach.[27] This differs from previously published work that described an interaction between VP24 and STAT1.[21] However, the difference in these results may be due to different systems employed. In the previously published work, the interaction between EBOV VP24 and STAT1 was determined by ELISA using purified truncated forms of VP24 and STAT1.[21] In the present study, the EGFP moiety may have prevented interaction with STAT1, likewise with the tandem affinity approach described previously,[27] although the tag did not prevent interaction with the karyopherins and other cellular proteins.

Sec61α was not listed in the final data set, but proteins that form a complex with Sec61α were identified, including SSR4 and Sec61B. Notably, Sec61B has been formally demonstrated to be significant using biological approaches.[25] Indeed, Sec61B protein was found in one of the trial runs of this study but excluded after the statistical analysis of the five independent mass spectrometry analyses of EGFP-VP24 and VP24-EGFP. This suggests that in the case of Sec61B our selection criteria was too conservative or affected by the EGFP moiety or the interaction with Sec61α may be a weaker or more transient interaction than those listed in Table 1. Although, we note that the interaction between VP24 and Sec61α was identified using a tandem tagging approach of VP24[25] but was not identified in a more recent study.[27]

One cellular protein with a high binding ratio was ATP1A1, a Na+/K+-ATPase. The function of this protein is in establishing and maintaining Na$^+$ and K$^+$ electrochemical gradients across the plasma membrane and in cell signaling. Inhibiting the function of ATP1A1 with ouabain resulted in a decrease in progeny virus. Ouabain is used in treating atrial fibrillation and heart failure and has been demonstrated to have antiviral effect with other viruses including herpes simplex virus[28] and porcine reproductive and respiratory syndrome virus.[29] The effect of ouabain on ATP1A1 may not have had a direct effect on the relationship between ATP1A1 and VP24. For example, treatment of cells infected with human cytomegalovirus with ouabain prevented enlargement of cells that is associated with progeny virus production.[30] Nevertheless, the use of this small molecule to reduce progeny virus in Ebola-virus-infected cells illustrates how existing therapeutics can be repurposed for antiviral therapy. In the case of a natural infection in humans, even a modest reduction in viral progeny production in vivo may slow the virus sufficiently for the host immune response to mount a life-saving response.

To our knowledge, this is the first detailed interactome analysis of VP24 using quantitative proteomics to identify cellular proteins that have a high probability of interacting with VP24 and to eliminate or identify cellular proteins that potentially associate with a binding matrix used in immuno-precipitations. The current study complements previous work that used small molecules to inhibit the function of cellular proteins to disrupt Ebola virus biology. For example, S-adenosylhomocysteine hydrolase inhibitors were evaluated both in vitro and in vivo and were detrimental to Ebola virus infection.[22] Inhibition of heat shock protein 90 using 17-AAG disrupted Ebola biology in vitro[31] At the time of publication of this manuscript, the largest EBOV outbreak so far known is occurring in West Africa and has proved difficult to control; the "repurposing" of therapeutics to reduce virus infection may tip the balance between recovery and death.

Overall, the proteomic approach demonstrated how determining the interactome of viral proteins can be used to identify cellular proteins that play important roles in the virus lifecycle and therefore increase the repertoire of potential drugable targets. Resistance is a constant problem in developing antiviral therapy to target the function of viral proteins. Transiently targeting the function of host cell proteins crucial to virus biology offers an exciting new therapeutic avenue, with the potential to solve the problem of resistance, as pro-viral cellular proteins are evolutionarily static on the time scale of lytic virus replication as well as separated from the genome that would benefit from resistance.

■ AUTHOR INFORMATION

Corresponding Authors

*R.H.: E-mail: Roger.Hewson@phe.gov.uk. Tel: 01980 612100.
*J.A.H.: E-mail: julian.hiscox@liverpool.ac.uk. Tel: 0151 795 0222.

Notes

The authors declare no competing financial interest.

■ ACKNOWLEDGMENTS

■ REFERENCES

(1) Feldmann, F.; Feldmann, H. Ebola: facing a new transboundary animal disease? Dev. Biol. 2013, 135, 201−209.

(2) Weingartl, H. M.; Nfon, C.; Kobinger, G. Review of Ebola virus infections in domestic animals. Dev. Biol. 2013, 135, 211−218.

(3) Marsh, G. A.; Haining, J.; Robinson, R.; Foord, A.; Yamada, M.; Barr, J. A.; Payne, J.; White, J.; Yu, M.; Bingham, J.; Rollin, P. E.; Nichol, S. T.; Wang, L. F.; Middleton, D. Ebola Reston virus infection of pigs: clinical significance and transmission potential. J. Infect. Dis. 2011, 204 (Suppl 3), S804−S809.

(4) Mateo, M.; Carbonnelle, C.; Reynard, O.; Kolesnikova, L.; Nemirov, K.; Page, A.; Volchkova, V. A.; Volchkov, V. E. VP24 is a molecular determinant of Ebola virus virulence in guinea pigs. J. Infect. Dis. 2011, 204 (Suppl 3), S1011−S1020.

(5) Mateo, M.; Carbonnelle, C.; Martinez, M. J.; Reynard, O.; Page, A.; Volchkova, V. A.; Volchkov, V. E. Knockdown of Ebola virus VP24 impairs viral nucleocapsid assembly and prevents virus replication. J. Infect. Dis. 2011, 204 (Suppl 3), S892−S896.

(6) Watanabe, S.; Noda, T.; Halfmann, P.; Jasenosky, L.; Kawaoka, Y. Ebola virus (EBOV) VP24 inhibits transcription and replication of the EBOV genome. J. Infect. Dis. 2007, 196 (Suppl 2), S284−S290.

(7) Reid, S. P.; Valmas, C.; Martinez, O.; Sanchez, F. M.; Basler, C. F. Ebola virus VP24 proteins inhibit the interaction of NPI-1 subfamily karyopherin alpha proteins with activated STAT1. J. Virol. 2007, 81 (24), 13469−13477.

(8) Reid, S. P.; Leung, L. W.; Hartman, A. L.; Martinez, O.; Shaw, M. L.; Carbonnelle, C.; Volchkov, V. E.; Nichol, S. T.; Basler, C. F. Ebola virus VP24 binds karyopherin alpha1 and blocks STAT1 nuclear accumulation. J. Virol. 2006, 80 (11), 5156−5167.

(9) Randall, R. E.; Goodbourn, S. Interferons and viruses: an interplay between induction, signalling, antiviral responses and virus countermeasures. J. Gen. Virol. 2008, 89 (Pt 1), 1−47.

(10) Mateo, M.; Reid, S. P.; Leung, L. W.; Basler, C. F.; Volchkov, V. E. Ebolavirus VP24 binding to karyopherins is required for inhibition of interferon signaling. J. Virol. 2010, 84 (2), 1169−1175.

(11) Lee, M. S.; Lebeda, F. J.; Olson, M. A. Fold prediction of VP24 protein of Ebola and Marburg viruses using de novo fragment assembly. J. Struct. Biol. 2009, 167 (2), 136−144.

(12) Ramanan, P.; Shabman, R. S.; Brown, C. S.; Amarasinghe, G. K.; Basler, C. F.; Leung, D. W. Filoviral immune evasion mechanisms. Viruses 2011, 3 (9), 1634−1649.

(13) Mateo, M.; Carbonnelle, C.; Reynard, O.; Kolesnikova, L.; Nemirov, K.; Page, A.; Volchkova, V. A.; Volchkov, V. E. VP24 is a molecular determinant of Ebola virus virulence in guinea pigs. J. Infect. Dis. 2011, 204 (Suppl 3), S1011−S1020.

(14) Volchkov, V. E.; Chepurnov, A. A.; Volchkova, V. A.; Ternovoj, V. A.; Klenk, H. D. Molecular characterization of guinea pig-adapted variants of Ebola virus. Virology 2000, 277 (1), 147−155.

(15) Ebihara, H.; Takada, A.; Kobasa, D.; Jones, S.; Neumann, G.; Theriault, S.; Bray, M.; Feldmann, H.; Kawaoka, Y. Molecular determinants of Ebola virus virulence in mice. PLoS Pathog. 2006, 2 (7), e73.

(16) Boulon, S.; Ahmad, Y.; Trinkle-Mulcahy, L.; Verheggen, C.; Cobley, A.; Gregor, P.; Bertrand, E.; Whitehorn, M.; Lamond, A. I. Establishment of a protein frequency library and its application in the reliable identification of specific protein interaction partners. Mol. Cell. Proteomics 2010, 9 (5), 861−879.

(17) Trinkle-Mulcahy, L.; Boulon, S.; Lam, Y. W.; Urcia, R.; Boisvert, F. M.; Vandermoere, F.; Morrice, N. A.; Swift, S.; Rothbauer, U.; Leonhardt, H.; Lamond, A. Identifying specific protein interaction partners using quantitative mass spectrometry and bead proteomes. J. Cell Biol. 2008, 183 (2), 223−239.

(18) Wu, W.; Tran, K. C.; Teng, M. N.; Heesom, K. J.; Matthews, D. A.; Barr, J. N.; Hiscox, J. A. The interactome of the human respiratory syncytial virus NS1 protein highlights multiple effects on host cell biology. J. Virol. 2012, 86 (15), 7777−7789.

(19) Emmott, E.; Munday, D.; Bickerton, E.; Britton, P.; Rodgers, M. A.; Whitehouse, A.; Zhou, E. M.; Hiscox, J. A. The cellular interactome of the coronavirus infectious bronchitis virus nucleocapsid protein and functional implications for virus biology. J. Virol. 2013, 87 (17), 9486−9500.

(20) Jourdan, S. S.; Osorio, F.; Hiscox, J. A. An interactome map of the nucleocapsid protein from a highly pathogenic North American porcine reproductive and respiratory syndrome virus strain generated using SILAC-based quantitative proteomics. Proteomics 2012, 12 (7), 1015−1023.

(21) Zhang, A. P.; Bornholdt, Z. A.; Liu, T.; Abelson, D. M.; Lee, D. E.; Li, S.; Woods, V. L., Jr.; Saphire, E. O. The ebola virus interferon antagonist VP24 directly binds STAT1 and has a novel, pyramidal fold. PLoS Pathog. 2012, 8 (2), e1002550.

(22) Huggins, J.; Zhang, Z. X.; Bray, M. Antiviral drug therapy of filovirus infections: S-adenosylhomocysteine hydrolase inhibitors inhibit Ebola virus in vitro and in a lethal mouse model. J. Infect. Dis. 1999, 179 (Suppl 1), S240−S247.

(23) Spurgers, K. B.; Alefantis, T.; Peyser, B. D.; Ruthel, G. T.; Bergeron, A. A.; Costantino, J. A.; Enterlein, S.; Kota, K. P.; Boltz, R. C.; Aman, M. J.; Delvecchio, V. G.; Bavari, S. Identification of essential filovirion-associated host factors by serial proteomic analysis and RNAi screen. Mol. Cell. Proteomics 2010, 9 (12), 2690−2703.

(24) Trombley, A. R.; Wachter, L.; Garrison, J.; Buckley-Beason, V. A.; Jahrling, J.; Hensley, L. E.; Schoepp, R. J.; Norwood, D. A.; Goba, A.; Fair, J. N.; Kulesh, D. A. Comprehensive panel of real-time TaqMan polymerase chain reaction assays for detection and absolute quantification of filoviruses, arenaviruses, and New World hantaviruses. *Am. J. Trop. Med. Hyg.* **2010**, *82* (5), 954−960.

(25) Iwasa, A.; Halfmann, P.; Noda, T.; Oyama, M.; Kozuka-Hata, H.; Watanabe, S.; Shimojima, M.; Watanabe, T.; Kawaoka, Y. Contribution of Sec61alpha to the life cycle of Ebola virus. *J. Infect. Dis.* **2011**, *204* (Suppl 3), S919−926.

(26) Nanbo, A.; Watanabe, S.; Halfmann, P.; Kawaoka, Y. The spatio-temporal distribution dynamics of Ebola virus proteins and RNA in infected cells. *Sci. Rep.* **2013**, *3*, 1206.

(27) Pichlmair, A.; Kandasamy, K.; Alvisi, G.; Mulhern, O.; Sacco, R.; Habjan, M.; Binder, M.; Stefanovic, A.; Eberle, C. A.; Goncalves, A.; Burckstummer, T.; Muller, A. C.; Fauster, A.; Holze, C.; Lindsten, K.; Goodbourn, S.; Kochs, G.; Weber, F.; Bartenschlager, R.; Bowie, A. G.; Bennett, K. L.; Colinge, J.; Superti-Furga, G. Viral immune modulators perturb the human molecular network by common and unique strategies. *Nature* **2012**, *487* (7408), 486−490.

(28) Dodson, A. W.; Taylor, T. J.; Knipe, D. M.; Coen, D. M. Inhibitors of the sodium potassium ATPase that impair herpes simplex virus replication identified via a chemical screening approach. *Virology* **2007**, *366* (2), 340−348.

(29) Karuppannan, A. K.; Wu, K. X.; Qiang, J.; Chu, J. J.; Kwang, J. Natural compounds inhibiting the replication of Porcine reproductive and respiratory syndrome virus. *Antiviral Res.* **2012**, *94* (2), 188−194.

(30) Altamirano, A. A.; Fons, M. P.; Russell, J. M.; Cragoe, E. J., Jr.; Albrecht, T. Human cytomegalovirus infection increases the number of ouabain-binding sites in human fibroblasts. *Virology* **1994**, *199* (1), 151−159.

(31) Smith, D. R.; McCarthy, S.; Chrovian, A.; Olinger, G.; Stossel, A.; Geisbert, T. W.; Hensley, L. E.; Connor, J. H. Inhibition of heat-shock protein 90 reduces Ebola virus replication. *Antiviral Res.* **2010**, *87* (2), 187−194.